The Journal of Physiology

Ageing changes in biventricular cardiac function in male and female baboons (*Papio* spp.)

Anderson H. Kuo[1], Cun Li[2,3], Hillary F. Huber[2], Peter W. Nathanielsz[2,3] and Geoffrey D. Clarke[1,3]

[1] *Radiology Department, University of Texas Health Science Center, San Antonio, TX, USA*
[2] *University of Wyoming, Laramie, WY, USA*
[3] *Southwest Primate Research Center, San Antonio, TX, USA*

Edited by: Harold Schultz & Janna Morrison

Key points

- Life course changes in cardiovascular function in a non-human primate have been comprehensively characterized.
- Age-related declines in normalized left ventricular stroke volume and cardiac output were found with corresponding decreases in biventricular ejection fractions and filling rates.
- There were age-related decreases in male and female baboon normalized left ventricular myocardial mass index, which declined at similar rates.
- Systolic functional declines in right ventricular function were observed with age, similar to the left ventricle.
- Sex differences were found in the rates and directions of right ventricular volume changes along with decreased end-systolic right ventricular sphericity.
- The results validate the baboon as an appropriate model for translational studies of cardiovascular functional decline with ageing.

Abstract Previous studies reported cardiac function declines with ageing. This study determined changes in biventricular cardiac function in a well-characterized baboon model. Cardiac magnetic resonance imaging measured key biventricular parameters in 47 baboons (22 female, age 4–23 years). ANCOVA assessed sex and age changes with $P < 0.05$ deemed significant. Stroke volume, cardiac output and other cardiac functional parameters were normalized to body surface area. There were similar, age-related rates of decrease in male (M) and female (F) normalized left ventricular (LV) myocardial mass index (M: $-1.2\,g\,m^{-2}\,year^{-1}$, F: $-0.9\,g\,m^{-2}\,year^{-1}$). LV ejection fraction declined at $-0.96\%\ year^{-1}$ ($r = -0.43$, $P = 0.002$) and right ventricular (RV) ejection fraction decreased at $-1.2\%\ year^{-1}$ ($r = -0.58$, $P < 0.001$). Normalized LV stroke volume fell at $-1.1\,ml\,m^{-2}\,year^{-1}$ ($r = -0.47$, $P = 0.001$), normalized LV ejection rate at $-3.8\,ml\,s^{-1}\,m^{-2}\,year^{-1}$ ($r = -0.43$, $P < 0.005$) and normalized LV filling rate at $-4.1\ ml\ s^{-1}\ m^{-2}\ year^{-1}$ ($r = -0.44$,

Anderson Houyun Kuo obtained his BS in Chemical and Biomolecular Engineering from Georgia Institute of Technology and then received his MD from the University of Tennessee Health Science Center. In 2018 he completed his Radiology Residency and obtained a PhD in Radiological Science from the University of Texas Health Science Center in San Antonio. He is now in the Neuroradiology Fellowship program a Brigham and Women's Hospital in Boston, MA. His research interest lies in the role of development in ageing. His research is focused on elucidating changes that occur during the prenatal and perinatal period that impact growth trajectories and how they may be ameliorated or even exploited. He has previously studied the impact of fetal nutrition restriction on cardiovascular health in baboons and uses magnetic resonance spectroscopy to assess myocardial lipid deposition of these baboons in conjunction with laboratory assessments of metabolism.

DOI: 10.1113/JP276338

$P < 0.005$). Also, RV wall thickening fraction decreased with age (slope $= -1\%$ year^{-1}, $P = 0.008$). RV ejection rate decreased at -3.6 ml s^{-1} m^{-2} year^{-1} ($P = 0.002$) and the normalized average RV filling rate dropped at -3.7 ml s^{-1} m^{-2} year^{-1} ($P < 0.0001$). End-systolic RV sphericity index also dropped with age ($r = -0.33$, $P = 0.02$). Many observed changes parallel previously reported data in human and animal studies. These measured biventricular functional declines in hearts with ageing from the closest experimental primate species to man underscore the utility of the baboon model for investigating mechanisms related to heart ageing.

(Received 19 April 2018; accepted after revision 6 August 2018; first published online 25 August 2018)
Corresponding author G. D. Clarke: Department of Radiology, University of Texas Health Science Center at San Antonio, 7703 Floyd Curl Drive – MC 7800, San Antonio, TX 78229-3900, USA. Email: clarkeg@uthscsa.edu

Introduction

Cardiovascular disease (CVD) remains a leading cause of mortality in the USA, underlying one of every three causes of death (Mozaffarian *et al.* 2015). After a period of consistent decline, recent statistics suggest that heart disease mortality is increasing, at least in some UK and US subpopulations (Mensah *et al.* 2017). Epidemiological studies suggest that if all major forms of CVD were eliminated, life expectancy would rise by approximately 7 years, as opposed to 3 years for all cancers (Danaei *et al.* 2009). Also remarkable is the strong age dependence of CVD incidence, being almost ubiquitous in patients over the age of 80 with 84.7% prevalence in males and 85.9% in females (Mozaffarian *et al.* 2015). As the elderly population continues to grow, the burden of heart disease will likely increase.

Age-associated loss of heart function has been recognized for decades. With ageing, many subjects exhibit progressive decreases in ejection fraction and cardiac index, with wide variability among individuals. The fall in left ventricular (LV) systolic function is preceded by impairment of diastolic function. In parallel, right ventricular (RV) heart function also declines. These functional changes occur in concert with structural changes including loss of myocardial mass, the development of myocardial fibrosis and left ventricular remodelling. Along with increasing vascular stiffening, these processes combine to make individuals more susceptible to cardiovascular diseases such as hypertension, arrhythmias and systolic heart failure. At a tissue level, the physiological effects of ageing are related to increased cardiomyocyte size and accumulations of calcium and fat deposits, as well as fibrosis in cardiac muscles (Chiao *et al.* 2015). Key mechanisms leading to these conditions include the dysregulation of the renin–angiotensin–aldosterone system (Wang & Shah, 2015) and the gradual impairment of key processes associated with autophagy (Shirakabe *et al.* 2016). The sex of the individual also modulates changes in myocyte mitochondrial function during the ageing process (Vijay *et al.* 2015). These changes may predispose the older heart to various forms of heart failure, including heart failure with preserved ejection fraction, as well as progressive coronary artery disease.

Non-invasive imaging technologies allow quantitative assessment of functional and structural cardiac ageing. A previous cardiac magnetic resonance imaging (CMRI) study in humans showed that most clinical parameters of LV systolic/diastolic function are significantly and independently influenced by sex, age and body surface area (BSA) (Maceira *et al.* 2006*a*). These results largely confirm data obtained with echocardiography and tissue Doppler ultrasound, but sample sizes were not large enough for measuring sex dependence, and in human studies control of the subjects' environment is not possible. Comparative studies in non-human primates allow precise environmental control in research subjects to reduce confounds and improved our understanding of the physiology, metabolic features, and genetic and epigenetic mechanisms influencing CVD initiation and progression (Cox *et al.* 2017). Specifically, baboons have been used to study glucose metabolism, atherosclerotic plaque formation and hypertension (Vandenberg *et al.* 2009; Cox *et al.* 2017). Recent studies suggest that overall heart function declines with ageing in the baboon (Kuo *et al.* 2017*a*,*b*), but no studies have reported normative declines across the life course.

In this study, we examined the biventricular function and morphology of male and female baboons using CMRI, a clinically established method for evaluating cardiac health. We demonstrated the practicality and utility of the baboon as a model for cardiac ageing research. The current study provides the most comprehensive accumulation of changes in RV and LV function and structure changes with age and sex in any non-human primate model.

Methods

Ethical approval

All procedures were approved by the University of Texas Health Science Center and Texas Biomedical Research Institute Institutional Animal Care and Use Committees (IACUC) and conducted in Association for Assessment and Accreditation of Laboratory Animal Care approved

facilities. The IACUC is accredited by the Association for Assessment and Accreditation of Laboratory Animal Care International.

Animal model

Baboons (*Papio* species) were maintained in an outdoor group social environment and fed using an individual feeding system described previously in detail (Schlabritz-Loutsevitch *et al.* 2004). *Ad lib* Purina Monkey diet (12% energy from fat, 0.29% glucose, 0.32% fructose and energy content of 3.07 kcal g^{-1}) was provided. Four cohorts of healthy baboons of both sexes were studied, corresponding to adolescent (ADL, 7M/4F), young adulthood (YNG, 8M/8F), mid adulthood (MID, 4M/4F) and late adulthood (OLD, 6M/6F). While the exact baboon to human life-stage correlation remains to be further studied, age correlation from baboons to humans is approximately 1:4 with some slight adjustments across the life course, especially before puberty. No interventions other than routine examinations under anaesthesia were performed in these cohorts.

Blood pressure data were acquired with the Omron HBP-1300 professional blood pressure monitor, using either a small (17–22 cm) or a medium (22–32 cm) cuff as appropriate. Prior to blood pressure measurement, baboons were isolated and sedated with intramuscular ketamine injection (10 mg kg^{-1}). Each baboon was placed in the supine position and the cuff positioned on the upper left arm. Blood pressure measurements began within 6 min of anaesthesia induction. Six measurements were made on each subject. Each of the six readings per individual was separated by 1–2 min, with the cuff completely loosened between measures. Mean arterial pressure was calculated by the standard formula, composed of one part systolic blood pressure and two parts diastolic blood pressure.

Cardiac magnetic resonance imaging

Cardiac magnetic resonance imaging (MRI) was performed under general anaesthesia. Anaesthesia was induced with ketamine hydrochloride (12 mg kg^{-1}, I.M.) and maintained with isoflurane (0.8–1.0%, inhaled). To allow mechanical ventilation, endotracheal intubation was performed following anaesthesia induction. Body temperature was maintained with a custom-built feedback-regulated circulating water blanket. Continuous physiological parameter monitoring was done, to include measurements of rectal temperature, P_{O_2}, end-tidal P_{CO_2}, electrocardiogram, heart rate and respiratory rate as well as visual assessment for respiration, movement and mucosal coloration. Mechanical ventilation was performed at approximately 10 stroke min^{-1} and 120–180 ml $stroke^{-1}$. In limited sequence acquisition where breath hold was required, a brief interval of hyperventilation was performed followed by a short period of ventilation suspension, not exceeding 30 s in duration. Prompt resumption of ventilation support was achieved following breath holds. Mechanical ventilation and physiological monitoring were performed using MRI-compatible machines.

All studies were performed on a 3.0 T clinical MRI scanner (TIM Trio, Siemens Healthineers, Erlangen, Germany) with a six-channel anterior phased-array torso coil and corresponding posterior spine coil elements, resulting in an aggregate of up to 12 channels of data. Before each imaging session, a standard quality control phantom was scanned. Functional CMRI was performed using steady-state free precession CMRI sequences. High temporal resolution cine CMRI with retrospective gating was performed (repetition time (TR)/echo time (TE) 3.0/1.5 ms, 25 cardiac phases, matrix 144 × 192, field of view 188 × 250 mm^2). Two five-slice, cine long-axis data sets, in a right anterior oblique view and a four-chamber view, were acquired. Afterwards, a set of 20–24 contiguous short-axis slices (2.5 mm thickness, no gap) was acquired serially during repetitive breath-holds at end expiration.

Following the CMRI session, inhalational isoflurane was discontinued, and the subject slowly weaned to room air and transported to the recovery area. Measurements of heart rate, electrocardiogram, temperature, blood pressure, P_{O_2}, and end-tidal CO_2 were repeated. After extubating, visual assessment of the animal for respiration, mucosal coloration and movement was performed at regular intervals not exceeding 15 min in duration until the time the animal was alert, in a sternal position, and demonstrated control of movement. After the experiments, the subjects were returned to the housing facilities.

Cardiac image analyses

Imaging data were analysed using the CMR[42] cardiac image analysis package (Circle Cardiovascular, Calgary, AB, Canada) using a standard method (Thiele *et al*, 2002). The LV endocardial and epicardial contours and RV endocardial contours were traced using a semi-automatic algorithm in a time-resolved manner, which resulted in a working biventricular model as previously described (Kuo *et al.* 2017*a*,*b*). End-diastolic volume (EDV) and end-systolic volume (ESV) were determined by maximum and minimum cavum volumes with visual confirmation. By convention, papillary muscles were included in the cavity volume. LV myocardial mass was estimated with empirical myocardial density (1.05 g ml^{-1}) and average of the LV myocardial volumes at end-systole and end-diastole. Stroke volume (SV = EDV − ESV) and cardiac output (CO = SV × heart rate) were determined in both right and left ventricles, then averaged. Ejection fraction (EF) was computed (EF = SV/EDV)

for the respective chamber. LV volume–time curves were assembled by calculating the LV volume for every phase of the cardiac cycle and plotting them out as a function of time after the QRS pulse measured by the electrocardiogram. Ejection and filling functions were assessed from the respective maximal downslope and upslope of the volume–time curves, giving peak LV ejection rate (PLVER) and peak LV filling rates (PLVFR). For example, PLVER was calculated as the maximum first derivative curve for LV ejection, which was determined by an iterative search for the maximum negative change in LV volume between end-diastole and end-systole. The rate of change in LV volume was calculated as:

$$\Delta V/\Delta t = (\mathrm{LVV}_x - \mathrm{LVV}_{x+1})/\mathrm{TR}$$

where LVV_x and LVV_{x+1} are the LV volumes of two adjacent data points on the LV volume curve and TR was the effective pulse repetition time (TR = 26.5 ms) used for cine CMRI. Biventricular average ejection and filling rates (AER, AFR) were obtained by dividing measured stroke volume by duration of systole and diastole. Segmentation of the LV was performed in accordance with the American Heart Association standard.

LV wall thickness (WT) was calculated using a three-dimensional algorithm developed to measure wall thickness always perpendicular to the myocardium (Holman *et al.* 1997). RV wall thickness was measured at the level of the mid-ventricular cavity in the lateral free wall at end-systole and end-diastole. To account for regional variability in wall thickness, measurements were taken from visually selected representative positions of the free wall within the slices, obtained from three consecutive slices, and averaged. Wall thickening fraction expressed in percentage (WTF) was defined as:

$$\mathrm{WTF} = (\mathrm{WT\text{-}ES} - \mathrm{WT\text{-}ED})/\mathrm{WT\text{-}ED} \times 100\%$$

where WT-ES is the wall thickness at end-systole and WT-ED is the wall thickness at end-diastole.

The three-dimensional sphericity index (SI) is used as an index of LV remodelling. The larger the SI, the more spherical the LV volume. SI is defined as the ratio of the LV volume to the volume of a sphere having the diameter of the LV major long axis (L_{es}), as measured from the mitral valve plane to the endocardial margin at the apex (Mannaerts *et al.* 2004; Kuo *et al.* 2017*a*). SI was determined both at end-systole (LV-ESSI) and end-diastole (LV-EDSI). For example, the end-diastolic sphericity index was calculated as:

$$\mathrm{LV\text{-}ESSI} = \mathrm{ESV}/[4/3\pi \cdot (L_{es}/2)^3]$$

The endocardial contour of the RV was traced to produce an RV model from which end-diastolic and end-systolic phases were determined as previously described (Kuo *et al.* 2017*b*). The length of the RV (L) was measured from the tricuspid plane to the chamber apex using long-axis images. The RV sphericity index was determined at both end-systole (RV-ESSI) and at end-diastole (RV-EDSI). For example, RV-ESSI was calculated as:

$$\mathrm{RV\text{-}ESSI} = \mathrm{RV\text{-}ESV}/[4/3\pi \cdot (L_{es}/2)^3]$$

where L_{es} is the length of the RV at end-systole (Kim *et al.* 2006).

Parameters based on dimensional measurements were evaluated with reference to the BSA. Heart dimensions were normalized to BSA because (1) that is the standard normalization method used in cardiac MRI studies in humans (Maceira *et al.* 2006*a*,*b*), and (2) BSA correlates strongly with measures, such as myocardial mass, in baboons (Kuo *et al.* 2017*a*,*b*). BSA was estimated using weight-based models as previously described for baboons (Vandeberg *et al.* 2009). For females:

$$\mathrm{BSA} = 0.078 \cdot \mathrm{Wt}^{0.664}$$

and in males,

$$\mathrm{BSA} = 0.083 \cdot \mathrm{Wt}^{0.639}$$

where BSA is given in meter squared with weight in kilograms.

Statistical analyses

Data were analysed using R 3.2.1 statistical software (R Foundation for Statistical Computing, Vienna, Austria) and Prism 6 (GraphPad Software Inc., La Jolla, CA, USA). Data are presented as mean ± standard deviation (SD), standard error of mean (SEM), or confidence interval (CI) as indicated. Scatter plots are constructed with estimated regression lines (continuous) and 95% confidence interval bands (dotted). Normality of data sets was assessed by the d'Agostino–Pearson test in a sex- and age-group-specific manner. Grubbs's test (extreme Studentized deviate) was performed to evaluate for statistical outliers. Baseline characteristics and cardiac timing parameters were evaluated using two-way ANOVA, with age group and sex as factors. One-way ANCOVA was used with numerical age as the independent variable and sex as the covariate to evaluate the CMRI-measured parameters with age as the independent variable and sex as covariate. In cases where the regression slope was not determined to be different between the sexes, the sexes were binned to increase power, and linear regression was used to evaluate the null hypotheses that there is no relationship between age and the analysed parameter. For cases in which ANCOVA could not be performed due to significant interaction between the grouping variable (age) and covariate, two-way analysis of variance (ANOVA) was performed. Probabilities are deemed significant at $P < 0.05$.

Table 1. Baseline characteristics of subjects studied

	ADL		YNG		MID		OLD	
Group	M	F	M	F	M	F	M	F
Number	7	4	8	8	4	4	6	6
Age (years)	3.1 ± 0.1	3.2 ± 0.1	5.4 ± 1.4	5.7 ± 1.3	10.4 ± 0.5	9.5 ± 0.3	18.2 ± 2.6	13.6 ± 1.4
Weight (kg)	10.7 ± 1.2	9.8 ± 0.8	19.5 ± 6.8	13.9 ± 2.1	33.9 ± 4.1	17.3 ± 2.0	31.4 ± 7.5	17.2 ± 2.2
Body surface area (m^2)	0.38 ± 0.03	0.36 ± 0.02	0.55 ± 0.12	0.45 ± 0.04	0.81 ± 0.07	0.51 ± 0.04	0.76 ± 0.12	0.51 ± 0.04

Data are means ± SD. ADL, adolescent; MID, middle aged; OLD, older; YNG, young adult.

Table 2. Cardiac timing and blood pressure

	ADL		YNG		MID		OLD		ANOVA
Group	M	F	M	F	M	F	M	F	
Number	7	4	8	8	4	4	6	6	—
Heart rate (bpm)	95 ± 5	89 ± 6	95 ± 3	108 ± 6	99 ± 6	98 ± 10	89 ± 3	97 ± 5	—
Time in systole (ms)	296 ± 16	312 ± 15	253 ± 12	257 ± 22	273 ± 11	296 ± 33	277 ± 20	245 ± 12	—
Time in diastole (ms)	349 ± 30	374 ± 43	385 ± 10	309 ± 16	340 ± 40	339 ± 48	402 ± 15	386 ± 35	—
Diastole to systole ratio	1.2 ± 0.1	1.2 ± 0.1	1.6 ± 0.1	1.3 ± 0.1	1.3 ± 0.2	1.2 ± 0.1	1.5 ± 0.1	1.6 ± 0.2	OLD > ADL*
Systolic blood pressure (mmHg)	113 ± 4	119 ± 4	103 ± 5	124 ± 7	115 ± 9	109 ± 5	NA	NA	—
Diastolic blood pressure (mmHg)	61 ± 4	69 ± 11	53 ± 3	72 ± 3	60 ± 4	61 ± 6	NA	NA	—

Data are means ± SD. *$P < 0.05$. ADL, adolescent; MID, middle aged; NA, not available; OLD, older; YNG, young adult.

Results

Baseline data from the four baboon cohorts are shown in Table 1. We note again that age correlation from baboons to humans is approximate. Male baboons maintained higher body weight and BSA than females, a known physiological difference. Cardiac timing parameters and blood pressure data are shown in Table 2. Diastole-to-systole ratio was noted to be increased in the OLD baboons relative to the ADL group (1.54 ± 0.32 *versus* 1.20 ± 0.27, $P = 0.01$).

As in humans, stroke volume ($r = 0.75$, $P < 1 \times 10^{-6}$), cardiac output ($r = 0.63$, $P < 0.0001$), end-diastolic volume ($r = 0.75$, $P < 1 \times 10^{-7}$) and end systolic volume ($r = 0.81$, $P < 1 \times 10^{-8}$) were correlated with BSA. These results confirm that normalization of LV functional parameters to BSA is appropriate for baboon age and sex analyses. Regression results for LV myocardial mass and overall LV function data are shown in Table 3.

Myocardial mass of the male baboons was higher than that of the females, both prior to and following normalization to BSA (Table 3 and Fig. 1*A* and *B*). Age-related increase in myocardial mass was seen (Fig. 1*A*). This was not apparent for myocardial mass after normalization for BSA (the mass index; MI). ANCOVA found a significant difference overall with respect to male and female LV MI values (Sex: $P = 0.015$). LV MI in females ($r = -0.57$, slope $= -1.2$ g m^{-2} year^{-1}) decreased significantly ($P = 0.005$) and the difference between LV MI slopes for males and females was significant (male slope $= -0.9$ g m^{-2} year^{-1}, Age: $P = 2 \times 10^{-5}$).

A decrease in LV EF with age (-0.96 ± 0.30 % year^{-1}, $P < 0.005$) was seen without sex differences (Table 4 and Fig. 2*A*). Stroke volume was higher in the males, but not after accounting for BSA (Table 3). Absolute SV and cardiac output remained stable throughout life (Table 3). However, there was a steady age-related decrease in both normalized SV ($r = -0.52$, $P < 0.005$) and the cardiac index (CI), which is the BSA-normalized cardiac output ($r = -0.49$, $P < 0.005$) (Fig. 2*B* and 2*C*). The normalized LV ESV (Table 4) did not change but there was a mild decrease ($r = -0.35$, $P < 0.02$) in normalized LV EDV with advancing age (Fig. 2*D*). No between-sex difference in these values was noted.

The normalized peak LV ejection rate decreased significantly (slope $= -7.2$ ml s^{-1} m^2 year^{-1}, $P = 0.002$) with age (Table 4). Similar age-related decreases (slope $= -3.8$ ml s^{-1} m^2 year^{-1}, $P = 0.005$) were seen in the normalized ejection rate averaged over the cardiac cycle (Table 3 and Fig. 3*A*). The normalized peak LV filling rate decreased significantly (slope $= -10.8$ ml s^{-1} m^2 year^{-1}, $P = 0.0004$) with age and normalized average LV filling rate (slope $= -4.1$ ml s^{-1} m^2 year^{-1}, $P = 0.002$; Fig. 3*B*). There were no sex differences found for the normalized

Table 3. Left ventricle: myocardial mass and overall cardiac function

Parameter	Sex difference in slope	Sex difference in elevation	Age regression *P*	Age regression R^2	Age regression slope
Absolute values					
MM (g)	NS	M > F***	***	M: 0.337 F: 0.054	M: 1.55 F: 0.26
SV (mL)	NS	M > F***	NS		
CO (mL min^{-1})	NS	M > F**	NS		
AER (mL s^{-1})	NS	M > F***	NS		
AFR (mL s^{-1})	NS	M > F*	NS		
Normalized to BSA					
MM/BSA (MI) (g m^{-2})	NS	M > F***	***	M: 0.25 F: 0.30	M: −0.9 F: −1.2
SV/BSA (mL m^{-2})	NS	NS	***	0.22	−1.1
CO/BSA (mL min^{-1} m^{-2})	NS	NS	**	0.21	−0.1
AER/BSA (mL s^{-1} m^{-2})	NS	NS	**	0.15	−3.8
AFR/BSA (mL s^{-1} m^{-2})	NS	NS	**	0.19	−4.1

*$P < 0.05$; **$P < 0.01$; ***$P < 0.005$. AER, average ejection rate; AFR, average filling rate; BSA, body surface area; CO, cardiac output; MI, mass index; MM, myocardial mass; SV, stroke volume.

ejection and filling rates. Analysis of a surrogate marker for LV function, wall thickening fraction (WTF), revealed no significant decrease with age but mildly elevated values in males compared to females ($P = 0.009$; Table 4).

The right ventricle also showed functional impairment with age (Table 5). RV EF decreased with age (slope = −1.2% $year^{-1}$, $P = 2 \times 10^{-5}$) without sex differences (Fig. 4*A*), comparable to the LV EF. However, unlike the WTF in the LV, the RV WTF (Fig. 4*B*) decreased with age (slope = −1% $year^{-1}$, $P = 0.008$). Age-related decreases (slope = −3.6 ml s^{-1} m^2 $year^{-1}$, $P = 0.002$) also were observed in the normalized RV ejection rate averaged over the cardiac cycle (Table 5 and Fig. 3*C*) and the average RV filling rate (slope = −3.7 ml s^{-1} m^2 $year^{-1}$, $P < 0.0001$) normalized to BSA (Fig. 3*D*). Significant interactions between Sex and Age were found in the

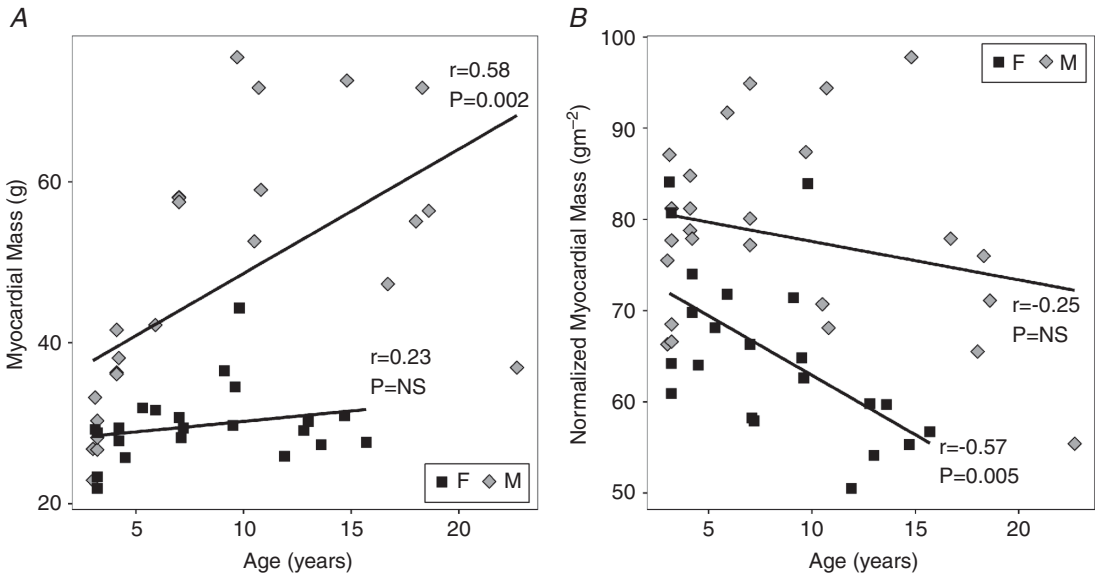

Figure 1. Left ventricular (LV) myocardial mass changes with age
A, significant differences ($P = 3 \times 10^{-4}$) in myocardial mass between male (M) and female (F) baboons were found, with significant increases occurring with age, particularly in males. However, the slopes were positive and the change with age was only significant in females. *B*, myocardial mass, normalized to body surface area (BSA), is also significantly different between males and females ($P = 2 \times 10^{-5}$) and decreases significantly with age ($P = 0.015$) in a manner that is most significant in females (slope = −1.2 g m^{-2} $year^{-1}$).

Table 4. Left ventricular function and morphology

Parameter	Sex difference in slope	Sex difference in elevation	Age regression *P*	Age regression R^2	Age regression slope (per year)
Absolute values					
LV EF (%)	NS	NS	**	0.19	−0.96
LV WTF (%)	NS	M > F**	NS		
LV ESV (mL)	NS	NS	***	0.19	0.60
LV EDV (mL)	NS	M > F**	*	0.10	0.79
LV ESSI (ratio)	NS	NS	NS	—	—
LV EDSI (ratio)	NS	NS	NS	—	—
LV PER (mL s^{-1})	NS	M > F***	NS	—	—
LV PFR (mL s^{-1})	NS	M > F*	NS	—	—
Normalized to BSA					
LV ESV/BSA (mL m^{-2})	NS	NS	NS	—	—
LV EDV/BSA (mL m^{-2})	NS	NS	*	0.12	−1.1
LV PER/BSA (mL s^{-1} m^{-2})	NS	NS	**	0.18	−7.2
LV PFR/BSA (mL s^{-1} m^{-2})	NS	M > F*	***	0.24	−10.8

*$P < 0.05$; **$P < 0.01$; ***$P < 0.005$. BSA, body surface area; EDSI, end-diastolic sphericity index; EDV, end-diastolic volume; EF, ejection fraction; ESSI, end-systolic sphericity index; ESV, end-systolic volume; PER, peak ejection rate; PFR, peak filling rate; WTF, wall thickening fraction.

RV ventricular volume data, which precluded the use of ANCOVA. ANOVA revealed that absolute RV ES and ED volumes remained stable in the females with age but increased in the males with age (Table 5). Significant increases in normalized RV ES volumes with age were found in males (slope = 0.98 ml m^2 $year^{-1}$, $P = 0.008$) but not in females (Fig. 5*A*). Concurrently, an age-related decline in normalized RV ED volumes was observed in the females (slope = −2.3 ml m^2 $year^{-1}$, $P = 0.008$) but not in the males (Fig. 5*B*).

Generally, a strong biventricular concordance in heart function with ageing was observed. LV and RV EF were strongly and positively correlated ($r = 0.44$, $P < 0.0001$). A positive correlation also was found for LV EF *versus* LV WTF ($r = 0.75$, $P < 0.0001$). A similar but weaker positive correlation as noted for RV EF *versus* RV WTF ($r = 0.50$, $P < 0.0004$). Given the strong coupling between RV and LV EF, normalized ejection rates were positively correlated with their respective LV EF and RV EF ($r_{LV} = 0.70$; $r_{RV} = 0.73$, $P < 0.0001$). The decline of EF with age in the left ventricle (−0.96 ± 0.30% $year^{-1}$) appears weaker than that of the right ventricle (−1.23 ± 0.26% $year^{-1}$) but was not significantly different. There were no significant changes in the LV ES and ED sphericity indexes with age and no sex difference (Table 4). In the right ventricle, the end-systolic sphericity index decreased with age (slope = −0.016% $year^{-1}$, $P = 0.02$) for both sexes while the RV end-diastolic SI was stable (Table 5 and Fig. 5*C*).

Discussion

The data collected in this study revealed age-related declines in stroke volume, normalized to BSA and cardiac index with corresponding decreases in biventricular ejection fraction and normalized ejection and filling rates in the ageing baboon. Related to these findings, we noted a mild decrease with age in MI and sex differences. These changes are subtle, and deviations of many measurements are not apparent prior to normalization to BSA (e.g. Fig. 1), which may partially explain the dissimilarities compared to some literature. Similar findings were apparent in both the right ventricle and the left, especially with regards to changes in ventricular volumes with ageing. There was a slight increase in LV spherical morphology at end-diastole with age, but unchanged end-systolic morphology while the RV sphericity index decreased significantly with ageing. Overall, many of these changes overlap with conditions that have been observed in humans, suggesting baboons are robust subjects for modelling human physiology.

Myocardial mass, mass index and morphology

The classical paradigm on cardiac ageing holds that there are age-related increases in ventricular wall thickness of the ageing human heart (Gertenblith *et al.*1977). This is based on the concept that cardiomyocyte hypertrophy and myocardial fibrosis, which occur with ageing, presumably leading to increased myocardial mass (Lakatta & Levy, 2003). Although there is general agreement that mass index (MI) is greater in human males than females, there have been divergent reports on the age-related changes in LV mass and LV MI (Cain, 2007). Early human autopsy studies reported decreased LV and RV myocardial mass and cardiomyocyte loss concurrent with age-related increases in LV wall thickness in men but not women

(Olivetti *et al.* 1991). These results are consistent with those in a later necropsy study in macaques (Zhang *et al.* 2007). CMRI studies have variously reported the absence of changes in both male and female MI values with age (Natori *et al.* 2006; Nikitin *et al.* 2006; Maceira *et al.* 2006*b*), reduced MI values in ageing hearts in males only (Hees *et al.* 2002) or reductions in LV MI without analysis of sex differentiation (Fiechter *et al.* 2013). Studies also have reported that LV MI declined in both sexes with increasing age (Cain *et al.* 2007; Cheng *et al.* 2009). In our baboon cohorts, there was a sex difference in MI, with tight, negative correlations of MI decreasing with age for each sex with a significant difference in the regression slopes (Table 3, Fig. 1*B*).

Human autopsy studies also have revealed that ventricular remodelling with age asymmetrically affects the interventricular septum and LV free wall, unaccompanied by a change in cardiac mass when normalized to BSA (Kitzman *et al.* 1988). Compensatory cardiac hypertrophy may occur normally in humans in response to the presence of cardiovascular disorders such as hypertension or coronary artery disease. However,

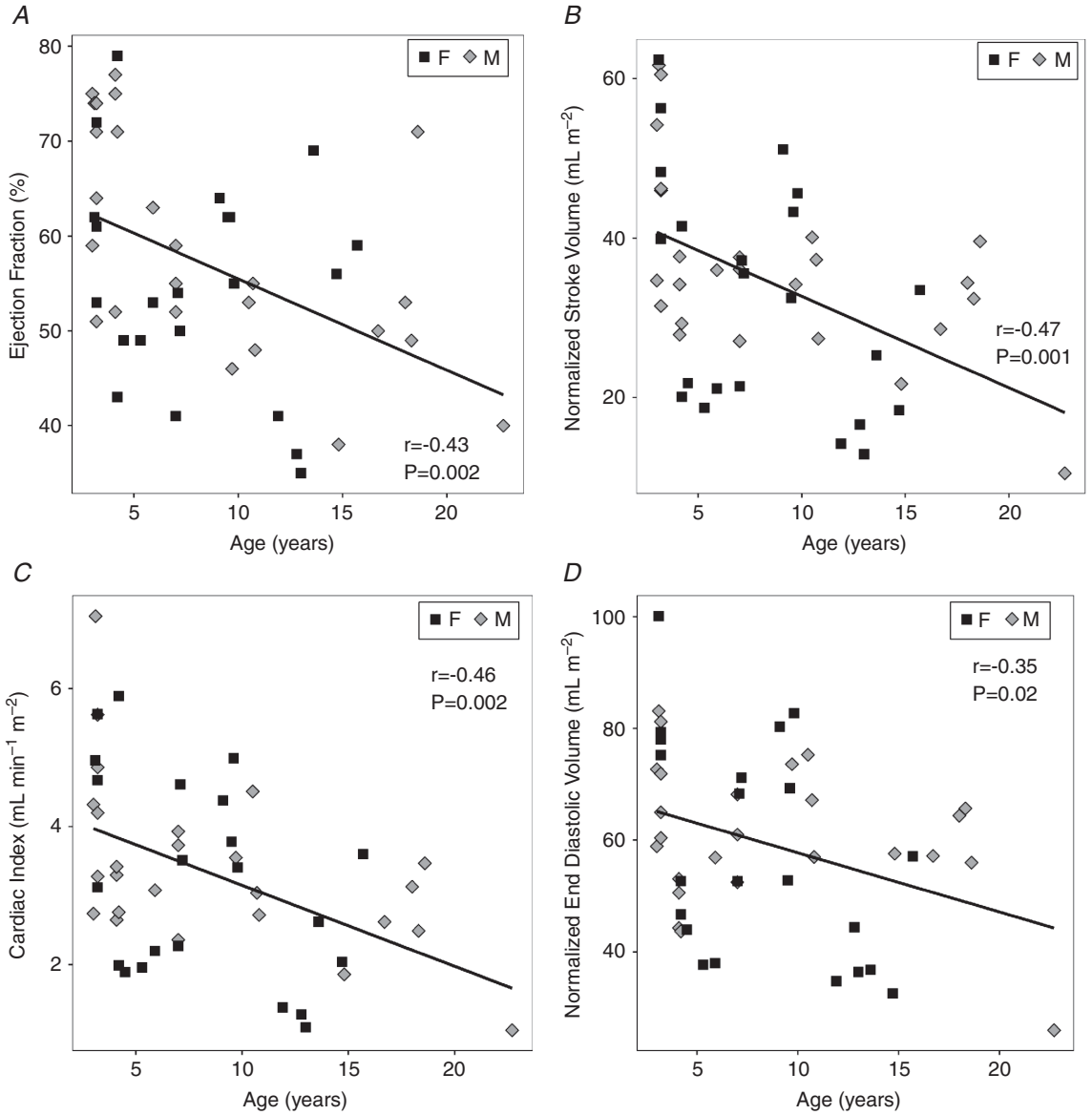

Figure 2. Left ventricular (LV) systolic function changes with age but without sex differences
A, the LV ejection fraction decreases significantly with age (slope = −1 % year^{-1}, $P = 0.002$). *B*, stroke volume, normalized to BSA, decreased with age (slope = −1.1 mL m^{-2} year^{-1}, $P = 0.001$). *C*, cardiac index also decreased with age (slope = −0.1 ml min^{-1} m^{-2} year^{-1}, $P = 0.002$). *D*, LV end diastolic volume, normalized to BSA, decreased with age (slope = −1.1 ml m^{-2} year^{-1}, $P = 0.02$). Linear regression (continuous line) was of data from male subjects (diamonds) and female subjects (squares).

neither factor was significant in our cohorts. Instead, our subjects were prone to a mild decrease in normalized cardiac mass.

Left ventricular function

Resting systolic function in human cardiac muscle is preserved overall with healthy ageing (Strait & Lakatta, 2012). Stable LV EF with age in humans has been reported by investigators using multiple imaging modalities (Onose *et al.* 1999; Lumens *et al.* 2006). A recent CMRI study on a population of humans even reported a minimal age-related increase in LV EF (Fiechter *et al.* 2013). However, the exclusion criteria for that study included an ejection fraction threshold, potentially excluding healthy subjects with physiologically low EF. We posit that a mild decrease in LV EF, seen in the current baboon study, likely does occur with age, even in humans, but may be

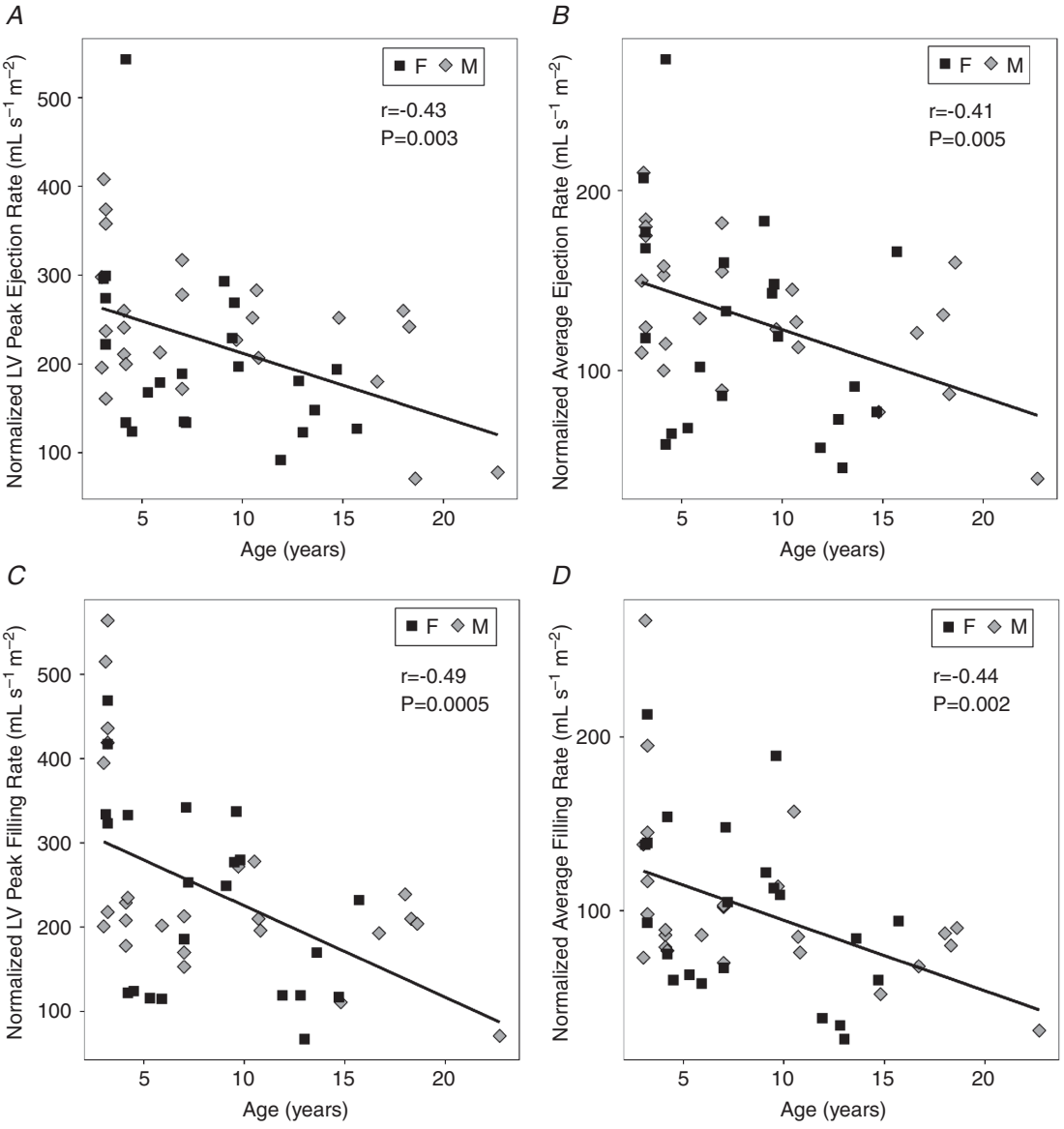

Figure 3. Changes in left ventricular (LV) and right ventricular (RV) systolic and diastolic function occurred with age
A, average LV ejection rate, normalized to BSA, significantly decreased with age (slope = −3.8 ml s^{-1} m^{-2} $year^{-1}$) but there were no significant differences between sexes. *B*, normalized average LV filling rate significantly decreased with age (slope = −3.8 ml s^{-1} m^{-2} $year^{-1}$) without a significant sex difference. *C*, average normalized RV ejection rate also was reduced with age (slope = −4.1 ml s^{-1} m^{-2} $year^{-1}$) and, *D*, there was an age-related decrease in normalized average RV filling rate (slope = −4.1 ml s^{-1} m^{-2} $year^{-1}$) without a significant sex difference for either parameter. Linear regression (continuous line) was of data from male subjects (diamonds) and female subjects (squares).

Table 5. Right ventricular function and morphology

Parameter	Sex difference in slope	Sex difference in elevation	Age regression *P*	Age regression R^2	Age regression slope
Absolute values					
RV EF (%)	NS	NS	***	0.33	−1.2
RV WTF (%)	NS	NS	**	0.15	−1.0
RV ESV (mL)†	*	—			
Male			***	0.39	1.2
Female			NS	—	—
RV EDV (mL)†	**	—		(Age: Sex interaction, $P = 0.04$)	
Male			***	0.33	1.5
Female			NS	—	—
RV ESSI (ratio)	NS	NS	*	0.11	−0.016
RV EDSI (ratio)	NS	NS	NS	—	—
Normalized to BSA					
RV ESV/BSA (mL m^{-2}) †	*	—		(Age: Sex interaction, $P = 0.008$)	
Male			*	0.17	0.98
Female			NS	0.10	0.12
RV EDV/BSA (mL m^{-2}) †	**	—		(Age: Sex interaction, $P = 0.006$)	
Male			NS	4×10^{-5}	0
Female			***	0.32	−2.3
RV AER/BSA (mL s^{-1} m^{-2}) †	NS	NS	**	0.19	−3.6
RV AFR/BSA (mL s^{-1} m^{-2}) †	NS	NS	***	0.22	−3.7

†Two-way ANOVA performed due to significant interaction between grouping variable (Age) and covariate (Sex). *$P < 0.05$; **$P < 0.01$; ***$P < 0.005$. AER, average ejection rate; AFR, average filling rate; BSA, body surface area; EDSI, end-diastolic sphericity index; EDV, end-diastolic volume; EF, ejection fraction; ESSI, end-systolic sphericity index; ESV, end-systolic volume; WTF, wall thickening fraction.

difficult to detect in clinical studies without extensive controls for confounding factors. Many investigators have reported subtle changes of systolic dysfunction, such as impairment of fibre shortening (Onose *et al.* 1999), torsion (Lumens *et al.* 2006) and blunted tension/pressure development during contraction with age (Lakatta *et al.* 1975), suggesting our finding of decreased function has a mechanical basis. Age-related decreases in stroke

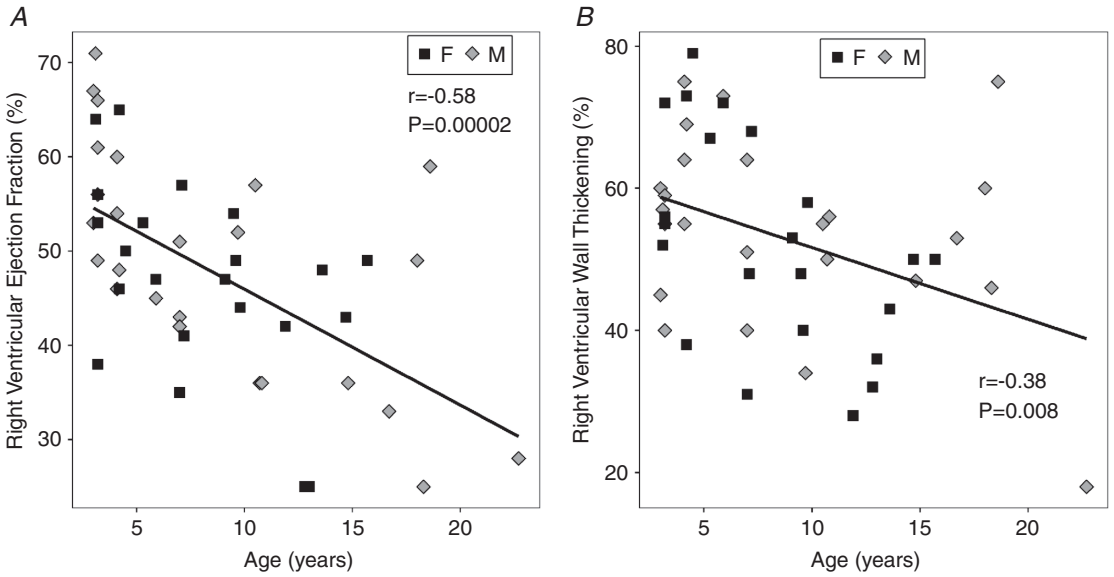

Figure 4. Right ventricular (RV) function became impaired with age
A, RV ejection fraction decreased with age (slope = −1.2% $year^{-1}$, $P = 2 \times 10^{-5}$). *B*, congruent findings were noted in RV wall thickening fraction (slope = −1% $year^{-1}$, $P = 0.008$). No sex effects were measured.

volume and cardiac output after normalization (Fig. 2*B* and *C*) are related findings. These results contrast with some of the human cardiac ageing literature, in which preserved stroke volume with age was reported (Lakatta & Levy, 2003). Similar changes have been reported in prior cardiac MRI ageing studies of healthy men and women (Hees *et al.* 2002; Nitikin *et al.* 2006; Cheng *et al.* 2009).

Similarly, decreased peak blood flow velocity and decreased flow acceleration have been reported downstream in the ascending aorta (Kelly *et al.* 1989). It is highly likely that these subtle systolic abnormalities contribute to diminished systolic capacity at rest, which become exacerbated during stress. It is known that peak ejection fraction during exercise decreases in older populations (Schulman *et al.* 1992). We note that even though LV WTF and LV EF are strongly correlated in the present study ($r = 0.75$, $P < 0.0001$), the decrease in LV WTF with age does not reach significance, further suggesting systolic decline may be difficult to detect.

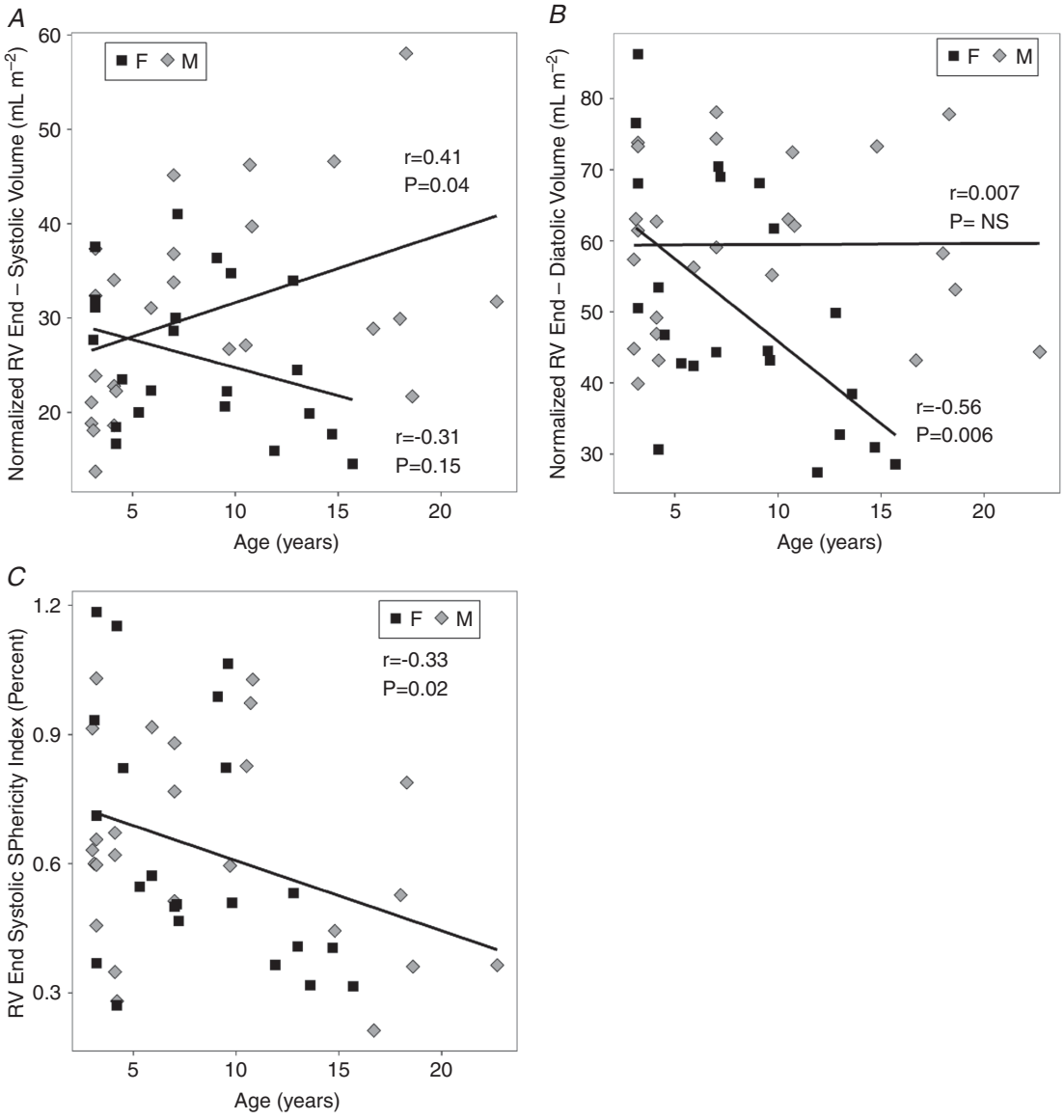

Figure 5. RV remodelling occurs with ageing
A, end-systolic RV volume, normalized to BSA, changed with age ($P = 0.0004$), exhibiting Sex:Age interactions ($P = 0.008$). RV ESV/BSA for males, but not for females, increased significantly with age (slope = 1 ml m^2 year^{-1}, $P = 0.04$). *B*, the opposite change with age in normalized end-diastolic RV volume was observed ($P = 0.0002$). RV ESV/BSA for females, but not males, decreased significantly with age (slope = −2.3 ml m^2 year^{-1}, $P = 0.006$. *C*, end-systolic sphericity index decreased with age (slope = −0.016, $P = 0.02$), without sex differences, but end-diastolic sphericity index did not change with age.

Our findings of gradual impairment of LV diastolic function, evidenced by decreases in normalized peak and average filling rates, are in line with the clinical and animal literature. Diminishing diastolic function is believed to originate from an age-dependent increase in cardiac fibrosis, which leads to stiffening of the ventricles. Rodent studies have confirmed the presence of cardiac fibrosis with age (Thomas *et al.* 2001). An inverse linear correlation between age and resting peak LV filling rate has been documented, which persists with exercise (Schulman *et al.* 1992). This is consistent with the results reported in the present study. Using CMRI tissue tagging, persistent rotation and torsion during myocardial relaxation and diastole have been noted in older subjects as well as a slower rate of fibre lengthening (Oxenham *et al.* 2003). A decrease in the filling rate in early diastole has been noted in older human subjects (Hollingsworth *et al.* 2012). Ultrasound studies have reported diastolic dysfunction with advancing age in the form of decreased mitral valve leaflet diastolic closure slope (E-F slope) (Olivetti *et al.* 1991), decreased early trans-mitral flow velocity and a decrease in the mitral early to late (E/A) flow ratio (Swinne *et al.* 1992). These changes persist with exercise and are thought to be intrinsic to the ageing heart, not explicable by other pathological changes or lack of training and exercise (Swinne *et al.* 1992; Kitzman *et al.* 1991). Relatedly, left atrial volume and amount of blood ejected during atrial systole increase with age (Triposkiadis *et al.* 1995). A multiple regression analysis identified the ratio of peak velocity blood flow from LV relaxation in early diastole to peak velocity flow in late diastole caused by atrial contraction (the E/A ratio) as the most powerful correlate of maximal oxygen consumption ($\dot{V}_{O_2max}$) in normal human subjects (Vanoverschelde *et al.* 1993). Additionally, multivariate analysis demonstrated that E/A $>$ 1.5 above baseline is associated with a twofold increase in all-cause mortality and a threefold increase in cardiac mortality independent of covariates (Bella *et al.* 2002). Preservation of LV diastolic function has been reported in a human study evaluating the effects of caloric restriction (Meyer *et al.* 2006).

Right ventricular function

Since the RV has a thinner wall and a more complex shape, i.e. triangular or crescentic depending on the viewing angle, evaluation of the RV chamber is more difficult (Taffet *et al.* 1997). This may contribute to the measured correlation of RV WTF with RV EF being weaker (r = 0.75 *vs.* r = 0.50) in the present study. The morphology of the RV is strongly dependent on LV health since the interventricular septum functionally belongs to the left ventricle. The age-related decrease in RV EF contradicts the human literature, in which RV EF is preserved or increased with advancing age secondary to decrease in both RV ESV and EDV (Kawut *et al.* 2011; Fiechter *et al.* 2013). In the present study, ES volume and ED volume demonstrated sexually dimorphic changes with age. In the females, both normalized RV ES and RV ED volumes were decreased, although only reaching significance at ED (Fig. 5*B*), whereas increased ES volumes were seen in the males (Fig. 5*A*). Despite these differences, RV ED sphericity index was stable and RV ES sphericity index decreased with age for both males and females (Fig. 5*C*). The measurement of reduced RV diastolic filling rate with age is consistent with the literature and similar to age-related changes found in the LV (Kukulski *et al.* 2000).

Sex differences in cardiac ageing

Differences in cardiac functional changes with ageing between sexes are subtle but appear biologically significant. Figure 6 compares the BSA-normalized LV volume–time curves over the cardiac cycle for males and females in the ADL and OLD groups. These data were first averaged over the 25–30 heartbeats of the CMRI scan for each subject and then averaged over all animals in each group. In older males, there is a tendency towards larger LV volume and an extension of the duration of systole (Fig. 6A). In females the left ventricular volume tends to decrease, and the overall R–R interval is increased, with a substantial increase in the duration of diastole over systole (Fig. 6B). A similar process with increased normalized RV volume in males and reduced RV volume in females apparently occurs in the right ventricle (Fig. 5).

There were some indications that subjects in the ADL group had not reached full maturity with respect to heart function. With the ADL group included, sphericity indices were stable. However, in the ADL group, highly variable LV morphology was noted at end-diastole. With the ADL group omitted, females had lower initial values of LV MI (YNG:F, 66.3 $\pm$ 5.9 g m^{-2}; MID:F, 70.7 $\pm$ 9.6 g m^{-2}) than males, which decreased significantly (F = 7.7, P = 0.005) with age (OLD:F 56.0 $\pm$ 3.5 g m^{-2}). A significant change in LV MI with age was not found (F = 1.3, P = 0.31) in males (YNG:M, 83.3 $\pm$ 6.6 g m^{-2}; MID:M, 80.2 $\pm$ 12.8 g m^{-2}; OLD:M, 74.0 $\pm$ 14.2 g m^{-2}). Without considering the ADL group, a more consistent LV spherical morphological trend was apparent, which revealed an increase in LV end-diastolic sphericity with advancing age (r = 0.53, $P < 0.005$). This morphological transition of the LV to a more globular form with post-adolescent ageing is suggestive of structural remodelling. Across all ages the systolic LV sphericity index was inversely correlated with the RV sphericity index at end-systole (r = −0.47, P = 0.0009). However, there was a positive correlation between the RV and LV sphericity indexes at end-diastole (r = 0.38, P = 0.008). These associations suggest that the heart's adaptations to maintain LV function through remodelling in normal ageing may have some impact on right ventricular systolic function.

It is possible that right ventricular remodelling may be a factor in the well-documented increase in systolic pulmonary artery pressure and vascular resistance that occur with ageing (Davidson & Fee, 1990; Armstrong *et al.* 2010). These changes are believed to be primarily due to a general increase in pulmonary arterial stiffness (Haddad *et al.* 2008). Future studies should be undertaken in these baboon cohorts to evaluate direct, mechanistic relationships between changes in RV morphology and function with regard to the pulmonary vascular changes that occur with ageing.

Summary

This study has several limitations. The animals were studied under anaesthesia, which requires careful monitoring and adjustment to maintain stable heart rate and blood pressure. Blood pressure measurements were not available for the OLD group. Only resting values of heart function were studied, which constrains full characterization of the cardiovascular system since only a fraction of the cardiovascular capacity is utilized at rest. Given that maximal exercise capacity has been shown to decrease with age (Lakatta & Levy, 2003), adding pharmacological stress during CMRI scanning (i.e. adenosine or dobutamine) would likely reveal more subtle deviations from normal cardiac function with ageing. This cross-sectional study revealed differences in cardiac function parameters with adequate effect sizes to produce significant results. However, longitudinal studies of the same animal would add considerable statistical power, and presumably, greater sensitivity to ageing changes. Fortunately, most of these subjects in the current project's cohorts remain alive and future measurements in the same subjects at different ages are still possible. In addition, advanced CMRI methods such as stress–strain analysis with tissue tagging, extracellular volume measurements with gadolinium contrast administration, and four-dimensional quantitative flow could significantly improve the scope and depth of our understanding of ageing-related changes in cardiac function.

Within primates, the old-world monkeys represent a superfamily that shares much similarity to humans. Baboons are the species closest to humans now that experimental studies on great apes are unavailable because of ethical concerns. In this regard, baboons (*Papio* spp.) are an asset to medical research. Important to cardiovascular research, baboons are omnivorous like humans, are terrestrial and exhibit forms of bipedalism. Metabolic syndrome and CVD spontaneously occur in primates (Vandeberg *et al.* 2009). They are also like humans in terms of development with generally singleton gestations, maternal nutrition load in pregnancy and lengthy neonatal nursing behaviour. Additionally, baboons are some of the largest primates, which is of importance considering the direct impact of body size upon cardiovascular demand. As in humans, morphometric methods have been examined and were shown to be predictive of body composition in the baboons, another advantage in this species (Vandeberg *et al.* 2009). Genetically, baboons' similarity to humans is evidenced at the overall DNA sequence level, individual gene sequence level, as well as chromosomal loci arrangement (Cox *et al.* 2017).

The life course data obtained in this study demonstrate that there are significant normative changes in both right and left ventricular heart function with ageing in the baboon, which generally correspond to the changes seen in human studies. Unlike in human studies, which are limited

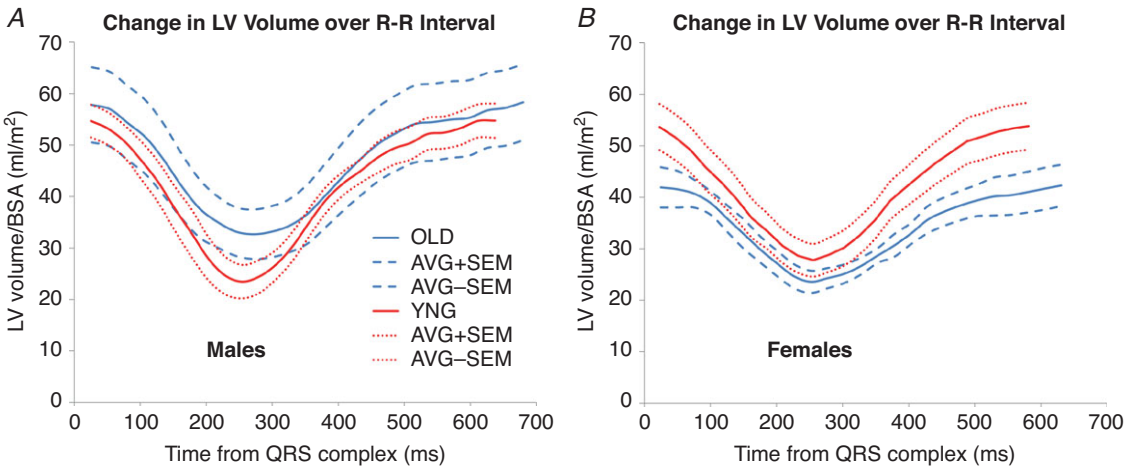

Figure 6. Sex differences were found in normalized LV time–volume curves across the cardiac cycle
A, for older males (blue lines), LV volumes tend to increase relative to younger animals (red lines). *B*, for females, LV volumes tend to decrease relative to younger subjects. Resting heart rate is slower for both sexes. Data represent average normalized LV volume (continuous lines) and mean ± SEM (dashed lines) for all animals in each group enumerated in Table 1.

by the difficulty in controlling for potential confounds, factors such as diet and amount and normality of the character of exercise have been well-controlled in this cohort. These normative data potentially could allow factors influencing biological *versus* chronological age to be identified. Generally, the CMRI results reported here support the baboon as a robust and appropriate model for studying the effects of ageing and its comorbidities, with the ability to produce useful information on the efficacy of various treatments that could be used in humans.

References

Armstrong DW, Tsimiklis G & Matangi MF (2010). Factors influencing the echocardiographic estimate of right ventricular systolic pressure in normal patients and clinically relevant ranges according to age. *Can J Cardiol* **26**, e35–e39.

Bella JN, Palmieri V, Roman MJ, Liu JE, Welty TK, Lee ET, Fabsitz RR, Howard BV & Devereux RB (2002). Mitral ratio of peak early to late diastolic filling velocity as a predictor of mortality in middle-aged and elderly adults: The Strong Heart Study. *Circulation* **105**, 1928–1933.

Cain PA, Ahl R, Hedstrom E, Ugander M, Allansdotter-Johnsson A, Friberg P, Marild S & Arheden H (2007). Physiological determinants of the variation in left ventricular mass from early adolescence to late adulthood in healthy subjects. *Clin Physiol Funct Imag* **27**, 254–262.

Cheng S, Fernandes VR, Bluemke DA, McClelland RL, Kronmal RA & Lima JA (2009). Age-related left ventricular remodeling and associated risk for cardiovascular outcomes: the multi-ethnic study of atherosclerosis. *Circ Cardiovasc Imag* **2**, 191–198.

Chiao YA & Rabinovitch PS (2015). The aging heart. *Cold Spring Harb Perspect Med* **5**, a025148.

Cox LA, Olivier M, Spradling-Reeves K, Karere GM, Comuzzie AG & VandeBerg JL (2017). Nonhuman primates and translational research—cardiovascular disease. *ILAR J* **58**, 235–250.

Danaei G, Ding EL, Mozaffarian D, Taylor B, Rehm J, Murray CJ & Ezzati M (2009). The preventable causes of death in the united states: Comparative risk assessment of dietary, lifestyle, and metabolic risk factors. *PLoS Med* **6**, e1000058.

Davidson WR & Fee EC 1990. Influence of aging on pulmonary hemodynamics in a population free of coronary artery disease. *Am J Cardiol* **65**, 1454–1458.

Fiechter M, Fuchs TA, Gebhard C, Stehli J, Klaeser B, Stähli BE, Manka R, Manes C, Tanner FC, Gaemperli O & Kaufmann PA (2013). Age-related normal structural and functional ventricular values in cardiac function assessed by magnetic resonance. *BMC Med Imag* **13**, 6.

Gerstenblith G, Frederiksen J, Yin FC, Fortuin NJ, Lakatta EG & Weisfeldt ML (1977). Echocardiographic assessment of a normal adult aging population. *Circulation* **56**, 273–278.

Haddad F, Hunt SA, Rosenthal DN & Murphy DJ (2008). Right ventricular function in cardiovascular disease, part I: Anatomy, physiology, aging, and functional assessment of the right ventricle. *Circulation* **117**, 1436–1448.

Hees PS, Fleg JL, Lakatta EG & Shapiro EP (2002). Left ventricular remodeling with age in normal men versus women: Novel insights using three-dimensional magnetic resonance imaging. *Am J Cardiol* **90**, 1231–1236.

Hollingsworth KG, Blamire AM, Keavney BD & Macgowan GA (2012). Left ventricular torsion, energetics, and diastolic function in normal human aging. *Am J Physiol Heart Circ Physiol* **302**, H885–H892.

Holman ER, Buller VG, de Roos A, van der Geest RJ, Baur LH, van der Laarse A, Bruschke AV, Reiber JH & van der Wall EE (1997). Detection and quantification of dysfunctional myocardium by magnetic resonance imaging: a new three-dimensional method for quantitative wall-thickening analysis. *Circulation* **95**, 924–931.

Kawut SM, Lima JA, Barr RG, Chahal H, Jain A, Tandri H, Praestgaard A, Bagiella E, Kizer JR, Johnson WC & Kronmal RA (2011). Sex and race differences in right ventricular structure and function: The MESA-right ventricle study. *Circulation* **123**, 2542–2551.

Kelly R, Hayward C, Avolio A & O'Rourke M (1989). Noninvasive determination of age-related changes in the human arterial pulse. *Circulation* **80**, 1652–1659.

Kim H, Kim Y, Park J, Kim KH, Kim K, Ahn H, Sohn D, Oh B, Park Y & Choi Y (2006). Determinants of the severity of functional tricuspid regurgitation. *Am J Cardiol* **98**, 236–242.

Kitzman DW, Scholz DG, Hagen PT, Ilstrump DM & Edwards WD (1988). Age-related changes in normal human hearts during the first 10 decades of life. Part II (Maturity): A quantitative anatomic study of 765 specimens from subjects 20 to 99 years old. *Mayo Clin Proc* **63**, 137–146.

Kitzman DW, Sheikh KH, Beere PA, Philips JL & Higginbotham MB (1991). Age-related alterations of Doppler left ventricular filling indexes in normal subjects are independent of left ventricular mass, heart rate, contractility and loading conditions. *J Am Coll Cardiol* **18**, 1243–1250.

Kukulski T, Hübbert L, Arnold M, Wranne B, Hatle L & Sutherland GR (2000). Normal regional right ventricular function and its change with age: A Doppler myocardial imaging study. *J Am Soc Echocardiogr* **13**, 194–204.

Kuo AK, Li C, Huber HF, Schwab M, Nathanielsz PW & Clarke GD (2017a). Maternal nutrient restriction during pregnancy and lactation leads to impaired right ventricular function in young adult baboons. *J Physiol* **595**, 4245–4260.

Kuo AK, Li C, Li J, Huber HF, Nathanielsz PW & Clarke GD (2017b). Cardiac remodeling in a baboon model of intrauterine growth restriction mimics accelerated aging. *J Physiol* **595**, 1093–1110.

Lakatta EG, Gerstenblith G, Angell CS, Shock NW & Weisfeldt ML (1975). Prolonged contraction duration in aged myocardium. *J Clin Invest* **55**, 61–68.

Lakatta EG & Levy D (2003). Arterial and cardiac aging: Major shareholders in cardiovascular disease enterprises: Part II: The aging heart in health: Links to heart disease. *Circulation* **107**, 346–354.

Lumens J, Delhaas T, Arts T, Cowan BR & Young AA (2006). Impaired subendocardial contractile myofiber function in asymptomatic aged humans, as detected using MRI. *Am J Physiol Heart Circ Physiol* **291**, H1573–H1579.

Maceira AM, Prasad SK, Khan M & Pennell DJ (2006a). Normalized left ventricular systolic and diastolic function by steady state free precession cardiovascular magnetic resonance. *J Cardiovasc Magn Reson* **8**, 417–426.

Maceira AM, Prasad SK, Khan M, Pennell DJ (2006b). Reference right ventricular systolic and diastolic function normalized to age, gender and body surface area from steady-state free precession cardiovascular magnetic resonance. *Euro Heart J* **27**, 2879–2888.

Mannaerts HF, van der Heide JA, Kamp O, Stoel MG, Twisk J & Visser CA (2004). Early identification of left ventricular remodelling after myocardial infarction, assessed by transthoracic 3D echocardiography. *Euro Heart J* **25**, 680–687.

Mensah GA, Wei GS, Sorlie PD, Fine LJ, Rosenberg Y, Kaufmann PG, Mussolino ME, Hsu LL, Addou E, Engelgau MM & Gordon D (2017). Decline in cardiovascular mortality: possible causes and implications. *Circ Res* **120**, 366–380.

Meyer TE, Kovács SJ, Ehsani AA, Klein S, Holloszy JO & Fontana L (2006). Long-term caloric restriction ameliorates the decline in diastolic function in humans. *J Am Coll Cardiol* **47**, 398–402.

Mozaffarian D, Benjamin EJ, Go AS, Arnett DK, Blaha MJ, Cushman M, De Ferranti S, Després JP, Fullerton HJ, Howard VJ & Huffman MD (2015). Executive summary: Heart disease and stroke statistics—2015 update. *Circulation* **131**, 434–441.

Natori S, Lai S, Finn JP, Gomes AS, Hundley WG, Jerosch-Herold M, Pearson G, Sinha S, Arai A, Lima JA & Bluemke DA (2006). Cardiovascular function in multi-ethnic study of atherosclerosis: normal values by age, sex, and ethnicity. *Am J Roentgenol* **186**, S357–S365.

Nikitin NP, Loh PH, de Silva R, Witte KK, Lukaschuk EI, Parker A, Farnsworth TA, Alamgir FM, Clark AL & Cleland JG (2006). Left ventricular morphology, global and longitudinal function in normal older individuals: a cardiac magnetic resonance study. *Intl J Cardiol* **108**, 76–83.

Olivetti G, Melissari M, Capasso JM & Anversa P (1991). Cardiomyopathy of the aging human heart. myocyte loss and reactive cellular hypertrophy. *Circ Res* **68**, 1560–1568.

Onose Y, Oki T, Mishiro Y, Yamada H, Abe M, Manabe K, Kageji Y, Tabata T, Wakatsuki T & Ito S (1999). Influence of aging on systolic left ventricular wall motion velocities along the long and short axes in clinically normal patients determined by pulsed tissue Doppler imaging. *J Am Soc Echocardiogr* **12**, 921–926.

Oxenham HC, Young AA, Cowan BR, Gentles TL, Occleshaw CJ, Fonseca CG, Doughty RN & Sharpe N (2003). Age-related changes in myocardial relaxation using three-dimensional tagged magnetic resonance imaging: structure and function. *J Cardiovasc Magn Reson* **5**, 421–430.

Schlabritz-Loutsevitch NE, Howell K, Rice K, Glover EJ, Nevill CH, Jenkins SL, Bill Cummins L, Frost PA, McDonald TJ & Nathanielsz PW (2004). Development of a system for individual feeding of baboons maintained in an outdoor group social environment. *J Med Primatol* **33**, 117–126.

Schulman SP, Lakatta EG, Fleg JL, Lakatta L, Becker LC & Gerstenblith G (1992). Age-related decline in left ventricular filling at rest and exercise. *Am J Physiol* **263**, H1932–H1938.

Shirakabe A, Ikeda Y, Sciarretta S, Zablocki DK & Sadoshima J (2016). Aging and autophagy in the heart. *Circ Res* **18**, 1563–1576.

Strait JB & Lakatta EG (2012). Aging-associated cardiovascular changes and their relationship to heart failure. *Heart Fail Clin* **8**, 143–164.

Swinne CJ, Shapiro EP, Lima SD & Fleg JL (1992). Age-associated changes in left ventricular diastolic performance during isometric exercise in normal subjects. *Am J Cardiol* **69**, 823–826.

Taffet GE, Pham TT & Hartley CJ (1997). The age-associated alterations in late diastolic function in mice are improved by caloric restriction. *J Gerontol A Biol Sci Med Sci* **52**, B285–B290.

Thiele H, Paetsch I, Schnackenburg B, Bornstedt A, Grebe O, Wellnhofer E, Schuler G, Fleck E & Nagel E (2002). Improved accuracy of quantitative assessment of left ventricular volume and ejection fraction by geometric models with steady-state free precession. *J Cardiovasc Magn Reson* **4**, 327–339.

Thomas PD, Cotter TA, Li X, McCormick RJ & Gosselin LE (2001). Exercise training attenuates aging-associated increases in collagen and collagen crosslinking of the left but not the right ventricle in the rat. *Eur J Appl Physiol* **85**, 164–169.

Triposkiadis F, Tentolouris K, Androulakis A, Trikas A, Toutouzas K, Kyriakidis M, Gialafos J & Toutouzas P (1995). Left atrial mechanical function in the healthy elderly: New insights from a combined assessment of changes in atrial volume and transmitral flow velocity. *J Am Soc Echocardiogr* **8**, 801–809.

Vandeberg JL, Williams-Blangero S & Tardif SD (2009). *The Baboon in Biomedical Research*. Springer Science & Business Media, New York.

Vanoverschelde JJ, Essamri BA, Vanbutsele R, d'Hondt A, Cosyns JR, Detry JR & Melin JA (1993). Contribution of left ventricular diastolic function to exercise capacity in normal subjects. *J Appl Physiol* **74**, 2225–2233.

Vijay V, Han T, Moland CL, Kwekel JC, Fuscoe JC & Desai VG (2015). Sexual dimorphism in the expression of mitochondria-related genes in rat heart at different ages. *PloS One* **10**: e0117047.

Wang M & Shah AM (2015). Age-associated pro-inflammatory remodeling and functional phenotype in the heart and large arteries. *J Mol Cell Cardiol* **83**, 101–111.

Zhang XP, Vatner SF, Shen YT, Rossi F, Tian Y, Peppas A, Resuello RR, Natividad FF & Vatner DE (2007). Increased apoptosis and myocyte enlargement with decreased cardiac mass; distinctive features of the aging male, but not female, monkey heart. *J Mol Cell Cardiol* **43**, 487–491.

Additional information

Competing interests

None of the authors has any conflicts of interest to disclose.

Author contributions

A.H.K. participated in the design of the work, the acquisition, analysis and interpretation of data for the work, and drafting the work and revising it critically for important intellectual content. C.L. participated in the design of the work, animal management, data acquisition and revising the manuscript critically for important intellectual content. H.F.H. participated in the design of the work, animal management, data acquisition and analysis, and in revising the manuscript critically for important intellectual content. P.W.N. participated in the conception and design of the work, animal management, interpretation of data and in revising the manuscript critically for important intellectual content. G.D.C. participated in the conception and design of the work, data analysis, interpretation of data, and in writing and revising the manuscript. All authors approved the final version of the manuscript, agree to be accountable for all aspects of the work in ensuring that questions related to the accuracy or integrity of any part of the work are appropriately investigated and resolved. All persons designated as authors qualify for authorship, and all those who qualify for authorship are listed.

Funding

This work was supported by the National Institutes of Health 5R24RR021367 (P.W.N.), 5R24OD010916 (P.W.N.), 5P01HD021350 (P.W.N.), 5R24OD011183 (P.W.N.), 5K25DK089012 (G.D.C.) and 1R25EB016631 (H.K.). NIH grant P51 OD011133 to the Southwest National Primate Centre was from the Office of Research Infrastructure Programs/Office of the Director. This work was also supported in part by funding from the EU FP 7/HEALTH/GA No.: 279281: BrainAge – Impact of Prenatal Stress on BRAINAGEing.

Acknowledgements

The authors thank Dr Robert Lanford and the Southwest National Primate Centre Staff for their ongoing support of the baboon research programme described in this article. The authors also acknowledge the technical support of Steven Rios, Sam Vega and Susan Jenkins, as well as the administrative support of Karen Moore.